JOURNAL OF GEOPHYSICAL RESEARCH VOL. 75, NO. 8, MARCH 10, 1970

Stress Estimates for South American Shallow and Deep Earthquakes[1]

MAX WYSS

Seismological Laboratory, California Institute of Technology
Pasadena, California 91109

Amplitude spectra of long-period mantle and body waves were used to obtain seismic moments for 37 earthquakes associated with the South American trench system. Corresponding seismic energies were estimated from the spectral densities of short-period P waves and also from the Gutenberg energy-magnitude relation. The apparent average stress (efficiency times average stress) in the source region was obtained from the ratio of energy to moment. The apparent average stress is a lower bound for the actual average stress. Near the surface a mean value for the apparent average stress is 18 bars. The mean value for depths between 45 and 150 km is 270 bars. Around 600 km depth the mean value is very similar to that at the surface, 21 bars. Differences in apparent average stress most likely reflect differences in strength of the material in the source region. The pattern of strength versus depth can be explained by ocean floor consumption. As lithospheric material plunges underneath oceanic trenches, it reaches higher pressures but is heated very slowly and thus will have relatively high strength until the temperature rises enough to weaken it. Comparison of the apparent average stress with estimates of the stress drop indicates an upper bound of about 0.1 for the seismic efficiency of deep and intermediate earthquakes.

INTRODUCTION

Recent applications of dislocation theory to earthquakes have led to the possibility of estimating absolute stress from the spectra of seismic waves. The amplitude of long-period waves is proportional to the seismic moment which, in turn, is proportional to the product of the average dislocation times the area of the dislocation [*Maruyama*, 1963; *Haskell*, 1964; *Aki*, 1966]. The amplitude of short-period waves, however, is more closely related to the energy released at the source which, in turn, is related to the average stress. If the energy is divided by the moment, the unknown product of average dislocation times dislocation area cancels out and the average stress acting in the source region is obtained [*Aki*, 1966; *Brune*, 1968; *Wyss and Brune*, 1968].

$$\frac{E}{M_0} = \frac{\langle\sigma\rangle A\langle u\rangle}{\mu A\langle u\rangle} = \frac{\langle\sigma\rangle}{\mu} = \langle\epsilon\rangle \qquad (1)$$

where

E is the elastic energy.
M_0 is the seismic moment.
$\langle\sigma\rangle = \frac{\sigma_1 + \sigma_2}{2}$ is the average stress (average of the initial and the final stress).
A is the fault plane area, dislocation area.
$\langle u\rangle$ is the mean relative displacement on A, average dislocation.
μ is the shear modulus.
$\langle\epsilon\rangle$ is the average shear strain.

The first average stress estimated in this way was obtained for the Niigata earthquake by *Aki* [1966], who pointed out the usefulness of the method for the study of deep earthquakes.

The total released energy is, however, not accessible to measurements. A lower bound for it can be obtained by determining the energy radiated to great distances in the form of seismic waves. Some energy will be dissipated as heat in the source region, and some of the high-frequency seismic radiation will be dissipated completely before it reaches teleseismic distances. The seismic energy E_s contained in frequencies between 0 and 1 hertz measured at teleseismic distances can be defined as the pro-

[1] Contribution 1629, Division of Geological Sciences, California Institute of Technology, Pasadena.

duct of the seismic efficiency factor η and the total energy produced by the dislocation

$$E_s(1) = \eta E \qquad (2)$$

Dividing the seismic energy by the moment gives a quantity defined as the apparent average strain.

$$E_s/M_0 = \eta\langle\epsilon\rangle = \eta\langle\sigma\rangle/\mu \qquad (3)$$

The apparent shear stress of the source region is obtained by multiplying the apparent shear strain by the shear modulus. The parts of the mantle where earthquakes occur must be different in composition and temperatures from the rest of the mantle. However, even for severe differences in these properties, the shear modulus would not change more than about 10%. To compute the stress it is an adequate approximation to use the shear moduli for corresponding depths in the mantle given by *Bullen* [1963]. The apparent average strains and stresses are a lower bound for the average strains and stresses.

Most of the seismically radiated energy is contained in the short-period waves. For most earthquakes under magnitude 7, the energy represented by waves with periods longer than 5 sec is negligible in comparison with the energy associated with waves between 1 and 2 sec period. The seismic energy of an earthquake is a strong function of the amplitude at the short-period end of the seismic spectrum. At long periods the spectral amplitudes of an earthquake tend to reach a constant value. The amplitude level at the long-period end of the spectrum is determined by the seismic moment. The ratio of high- to low-frequency spectral amplitudes is a direct measure of the apparent strain in the source region. The apparent strain is the basic quantity determined in this paper. Even though it is often more convenient to think in terms of apparent stress, one should remember that the basic measurements yield apparent strain. It should be emphasized at this point that the word 'strain' (stress) in this paper always means nonhydrostatic strain (stress).

Studies of seismic spectra may thus lead to estimates of absolute stress, provided that other parameters influencing the seismic spectrum can be properly evaluated. The correction factors for attenuation, instrument response, effects of the free surface, radiation pattern, and geometrical spreading were applied. The most uncertain parameter is the seismic efficiency. *Berckhemer and Jacob* [1968] have fitted seismic spectra to theoretical spectra of P waves, deducing the fault area and stress drop under the assumption of a rupture velocity. By comparison of the apparent stress with the stress drop one can obtain a largest possible efficiency, since the initial stress had to be equal to or larger than the stress drop. The ratios of apparent stress to stress drop are approximately the same for earthquakes at intermediate and great depths. The fact that the maximal efficiency does not vary between intermediate and great depths could suggest that the efficiency also does not change with depth. The changes of apparent stress would then reflect directly changes of stress. The maximum of the apparent stresses occurs at depths of approximately 100 km. In the major parts of the South American deep seismic zone the mean value of 10 earthquakes between 45 and 150 km is 270 bars. This value is an order of magnitude larger than the values at 0 and 600 km depth. If the apparent stresses are divided by the maximal seismic efficiency of 0.2, the stresses at 100 km depth average approximately 3 kb. The fault dimensions corresponding to these high-stress earthquakes are extremely small, 2 to 10 km for earthquakes with body wave magnitude 7.0. Although it has not been possible to demonstrate conclusively that this result is not due to a variation of efficiency with depth, most of the change of apparent average stress with depth appears to be due to change of average stress with depth. If the variation of stress with depth is real, it can be explained by the pressure-temperature environment to which a descending slab of lithosphere, as proposed by *Isacks et al.* [1968], is exposed.

Data

Fault plane solutions. For an accurate estimate of the seismic moment and the seismically radiated energy, the fault plane solution of an earthquake has to be known. Thirty-seven earthquakes associated with the South American seismic zone were selected on the basis of location (Figure 1) and size, as well as of the quality of existing fault plane solutions. The source of the fault plane solution is given in the last column of Table 1.

SOUTH

Moments. The equivalent double-mic moment, as defined in the disloca of faulting [*Maruyama*, 1963], wa from spectral densities observed at Where it was possible, the moment mined from long-period mantle wav as from long-period P waves. For t waves, the far-field displacement for couple and the excitation functions *Ben-Menahem and Harkrider* [1964] to obtain seismic moment from Ray Love waves having periods between 7(sec. Geometrical spreading and at were accounted for, the latter by usi values given by *Ben-Menahem* [1965]

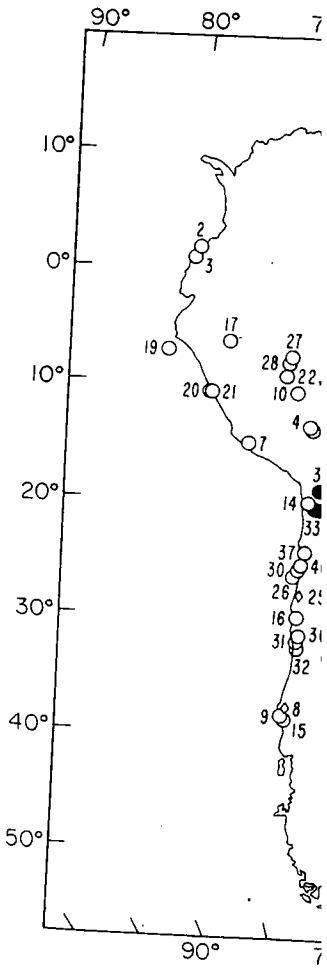

Fig. 1. Map of South America showi cate earthquakes outside main seismic z ally low apparent stresses.

Moments. The equivalent double-couple seismic moment, as defined in the dislocation theory of faulting [*Maruyama*, 1963], was obtained from spectral densities observed at Pasadena. Where it was possible, the moment was determined from long-period mantle waves as well as from long-period P waves. For the mantle waves, the far-field displacement for a double couple and the excitation functions given by *Ben-Menahem and Harkrider* [1964] were used to obtain seismic moment from Rayleigh and Love waves having periods between 70 and 150 sec. Geometrical spreading and attenuation were accounted for, the latter by using the Q values given by *Ben-Menahem* [1965]. For the P waves the far-field displacement for a double couple given by *Keilis-Borok* [1960] and *Ben-Menahem et al.* [1965] was used. The geometrical spreading and attenuation were accounted for by using a program described by *Julian and Anderson* [1968]. The results of *Ben-Menahem et al.* [1965] were used to compensate for the effects of the crust and the free surface. P waves having periods around 20 sec were used. In Table 2 the moments obtained from mantle waves are given as M_0(surf) and the moments obtained from P waves are given as $M_0(P)$. The period of the surface wave on which the calculation was based is also given in Table 2.

For the 17 shocks where the moment was ob-

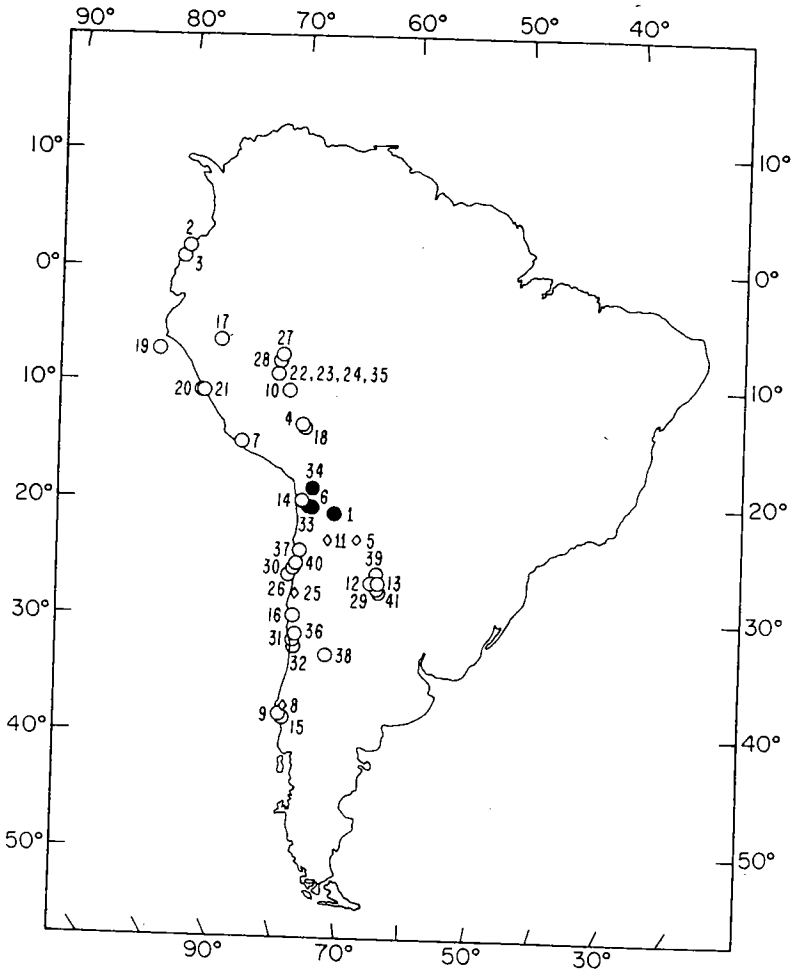

Fig. 1. Map of South America showing locations of earthquakes studied. Diamonds indicate earthquakes outside main seismic zone; full circles indicate earthquakes with exceptionally low apparent stresses.

Table 1. Earthquakes Selected for Study

Event	Date, d	m	y	Time h	m	s	Latitude S	Longitude W	Depth, km	Fault Mechanism Source*
1	29	11	57	22	19	41	21.0	67.0	190	(3)
2	01	02	58	16	10	15	−1.7	79.3	0	(3)
3	14	04	58	21	32	28	−1.0	79.5	0	(3)
4	26	07	58	17	37	13	13.5	69.5	630	(3)
5	12	05	59	09	46	55	23.2	65.0	26	(3)
6	14	06	59	00	12	02	20.4	69.0	83	(3)
7	15	01	60	09	30	19	15.0	75.0	70	(3)
8	22	05	60	10	32	43	37.5	73.0	0	(7)
9	20	06	60	02	01	09	38.2	72.8	0	(3)
10	31	08	61	01	48	39	10.4	70.7	605	(3)
11	03	08	62	08	56	12	23.2	67.5	71	(1)
12	29	09	62	15	17	48	27.0	63.6	575	(6)
13	08	12	62	21	27	18	27.0	63.0	620	(6)
14	29	12	62	10	41	04	20.0	69.9	46	(1)
15	05	02	63	20	39	22	38.4	73.2	41	(2)
16	10	03	63	10	51	48	29.9	71.2	70	(2)
17	13	04	63	02	20	58	6.2	76.5	125	(2)
18	15	08	63	17	25	06	13.8	69.3	543	(2)
19	29	08	63	15	30	31	7.1	81.6	23	(2)
20	17	09	63	05	54	34	10.6	78.2	61	(2)
21	24	09	63	16	30	16	10.6	78.0	80	(2)
22	09	11	63	21	15	30	9.0	71.5	575	(2)
23	10	11	63	01	00	39	9.2	71.5	600	(2)
24	11	11	63	19	54	09	9.1	71.4	585	(5)
25	25	07	64	19	31	07	27.9	70.9	26	(6)
26	18	08	64	04	44	58	26.4	71.5	8	(6)
27	28	11	64	16	41	33	7.7	71.2	626	(5)
28	28	11	64	16	49	30	8.0	71.4	655	(5)
29	09	12	64	13	35	42	27.5	63.2	580	(6)
30	23	02	65	22	11	50	25.7	70.5	40	(6)
31	22	03	65	22	56	26	31.9	71.5	80	(6)
32	28	03	65	16	33	16	32.4	71.3	72	(6)
33	12	06	65	18	50	12	20.5	69.3	102	(6)
34	20	08	65	09	42	49	18.9	69.0	128	(6)
35	03	11	65	01	39	03	9.1	71.4	590	(4)
36	10	04	66	16	36	14	31.5	71.2	64	(6)
37	27	07	66	04	48	59	24.2	70.3	35	(6)
38	10	11	66	03	02	32	31.9	68.4	120	(6)
39	20	12	66	12	26	55	26.1	63.2	589	(6)
40	28	12	66	08	18	07	25.5	70.7	47	(6)
41	09	09	67	10	06	44	27.7	63.1	578	(6)

* Key to fault mechanism source: (1) *Stauder and Bollinger* [1964]; (2) *Stauder and Bollinger* [19
(3) *Wickens and Hodgson* [1967]; (4) *Khattri* [1969]; (5) Earthquakes, for which the moment was obta
by *Berckhemer and Jacob* [1968]; (6) *Stauder* [1970].

tained by both surface waves and body waves, the values agree within a factor of 3 for all but two shocks; for them the agreement is within a factor of 4. This agreement is considered good. The moment determined by surface waves is considered more reliable because it is not as greatly affected by local crustal properties as the shorter-period body waves. If it was available, the moment determined from sur
waves was used for the strain and stress de
minations.

Energy. The estimation of energy is les
liable than the determination of moment.
major part of the observed seismic ener
associated with the body waves. The ampli
of these waves are subject to strong attenu

and effects of the local crustal struct
source and at the receiver. This unc
amplitude is very important because
is a function of the amplitude squared
previous studies involving seismic e
Gutenberg energy-magnitude formula
used [*Gutenberg and Richter*, 1956],
$5.8 + 2.4m$. However, the accurac
formula for deep earthquakes has
ascertained. In this study P-wave ene

TABLE 2. Seismic Mo

Event	h, km	T(surf), sec	M_0(surf), dyne cm 10^{26}	M_0 dyn 1
1	190	120	51.	78.
2	0	100	2.6	7.0
3	0	100	1.8	1.6
4	630	200	28.	...
5	26	100	0.96	1.9
6	83	100	5.9	11.4
7	70	100	2.0	8.0
8	0	100	1.7	...
9	0	100	3.8	...
10	605	...	...	8.3
11	71	100	2.3	2.3
12	575	...	...	1.5
13	620	200	12.	3.8
14	46	100	0.3	0.6
15	41	100	0.64	...
16	70	30	0.03	...
17	125	100	0.26	1.0
18	543	200	140.	...
19	23	100	5.2	...
20	61	85	0.11	...
21	80	85	2.0	3.0
22	575	240	7.4	8.3
23	600	...	...	0.32
24	585	...	...	0.00
25	26	100	0.53	0.74
26	8	70	3.7	...
27	626	...	...	0.097
28	655	...	...	0.079
29	580	100	0.3	0.87
30	40	70	4.2	3.0
31	80	70	0.063	...
32	72	100	5.4	6.6
33	102	100	0.1	...
34	128	100	1.6	...
35	590	...	...	1.2
36	64	100	...	0.08
37	35	70	0.1	...
38	120	70	0.15	...
39	589	...	...	0.38
40	47	100	23.	18.
41	578	...	...	0.87

Berckhemer and Jacob [1968].

and effects of the local crustal structure at the source and at the receiver. This uncertainty in amplitude is very important because the energy is a function of the amplitude squared. In many previous studies involving seismic energy, the Gutenberg energy-magnitude formula has been used [*Gutenberg and Richter*, 1956], $\log E = 5.8 + 2.4m$. However, the accuracy of this formula for deep earthquakes has not been ascertained. In this study P-wave energies were estimated from spectral analysis of seismograms, and it was concluded that the Gutenberg-Richter energy-magnitude relation provides a good estimate, even for deep shocks.

The energies determined in this study are based on the energies carried by the P waves. The amplitudes of the S waves are generally about 3 times larger than those of the P waves [*Haskell*, 1964; *Archambeau*, 1964]. Since the energy in seismic waves is a function of the

TABLE 2. Seismic Moments, Apparent Strains, and Apparent Stresses

Event	h, km	T(surf), sec	M_0(surf), dyne cm 10^{26}	$M_0(P)$, dyne cm 10^{26}	m_b	$E_G(m_b)$, dyne cm 10^{21}	$10E_x(1)$, dyne cm 10^{21}	$\eta\bar{\epsilon}$ 10^{-5}	$\eta\bar{\sigma}$, bars	Quality
1	190	120	51.	78.	7.5	630.	...	12.4	91.	*B*
2	0	100	2.6	7.0	6.9	23.	...	8.8	26.	*B*
3	0	100	1.8	1.6	6.8	13.	...	7.2	22.	*B*
4	630	200	28.	...	6.9	25.	...	0.9	12.	*B*
5	26	100	0.96	1.9	7.0	40.	...	40.	120.	*B*
6	83	100	5.9	11.4	7.15	91.	70.	15.	102.	*B*
7	70	100	2.0	8.0	6.9	25.	11.	12.5	81.	*B*
8	0	100	1.7	...	7.2	120.	...	71.	210.	*B*
9	0	100	3.8	...	6.9	25.	...	6.6	20.	*B*
10	605	...	...	8.3	6.9	25.	36.	3.	39.	*B*
11	71	100	2.3	2.3	7.25	160.	...	70.	450.	*A*
12	575	...	...	1.5	6.5	2.5	2.4	1.7	22.	*B*
13	620	200	12.	3.8	6.6	4.3	3.4	0.5	7.	*A*
14	46	100	0.3	0.6	6.7	7.6	...	25.	170.	*A*
15	41	100	0.64	...	6.5	2.5	...	3.9	24.	*A*
16	70	30	0.03	...	6.3	0.8	0.7	26.6	173.	*B*
17	125	100	0.26	1.0	7.0	40.	44.	154.	1050.	*A*
18	543	200	140.	...	7.35	280.	100.	2.	24.	*A*
19	23	100	5.2	...	7.0	40.	...	7.7	23.	*A*
20	61	85	0.11	...	6.7	8.0	...	73.	470.	*A*
21	80	85	2.0	3.0	7.0	40.	14.	20.	132.	*A*
22	575	240	7.4	8.3	7.0	40.	...	5.4	70.	*A*
23	600	...	...	0.32*	6.3	0.8	...	2.5	33.	*A*
24	585	...	...	0.003*	5.4	0.0058	...	1.9	25.	*B*
25	26	100	0.53	0.74	6.7	7.6	...	14.3	43.	*A*
26	8	70	3.7	...	6.9	23.	...	6.2	19.	*A*
27	626	...	...	0.097*	5.6	0.017	...	0.18	2.	*B*
28	655	...	...	0.079*	5.6	0.017	...	0.22	3.	*B*
29	580	100	0.3	0.87	6.2	0.48	0.06	0.55	7.	*A*
30	40	70	4.2	3.0	6.75	10.	...	2.4	15.	*A*
31	80	70	0.063	...	6.4	1.5	...	23.	155.	*B*
32	72	100	5.4	6.6	7.2	120.	...	22.	145.	*A*
33	102	100	0.1	...	6.0	0.16	0.013	1.6	11.	*B*
34	128	100	1.6	...	6.3	0.52	...	0.33	2.	*A*
35	590	...	...	1.2	6.6	4.4	...	3.6	48.	*A*
36	64	100	...	0.08	6.0	0.16	...	2.0	13.	*B*
37	35	70	0.1	...	6.1	0.27	...	2.7	8.	*B*
38	120	70	0.15	...	6.4	1.5	...	10.	67.	*B*
39	589	...	...	0.38	5.85	0.069	...	0.18	2.	*B*
40	47	100	23.	18.	7.45	48.	...	2.1	13.	*A*
41	578	...	...	0.87	6.1	0.27	...	0.31	4.	*A*

* *Berckhemer and Jacob* [1968].

amplitude squared, the energy carried by the S waves is about 10 times larger than the P-wave energy. The attenuation of the P waves is less severe than that of S waves. Therefore the indirect estimate using the P-wave energy was preferred to a direct estimate of the S-wave energy. The spectral density of the P wave at 1 sec period was estimated from the records for the short-period vertical instruments at Pasadena by the formula

$$u = 2A(Tn/2\pi)$$

where u is the amplitude spectral density, A is the ground amplitude, T is the period, and n is the number of periods with amplitude A. The spectral densities between 100 and 5 sec period were also available from Fourier analysis of the Pasadena long-period records. The high-frequency waves account for most of the seismically radiated energy. For most earthquakes the energy associated with waves of lower frequencies than 0.5 hertz is much smaller than the energy traveling in a 1-hertz wave. For this reason it was considered to be a good approximation to assume that the amplitude spectral density was constant from ∞ to 1 sec period and equal to the spectral density at 1 sec period. If longer-period waves made an unusually large contribution, their energy was also accounted for. On this basis the lower bound for seismic energy called $E_p(1)$ is defined. All the energy that was produced at the source but was not accounted for in the described estimate is taken care of by the seismic efficiency factor η.

The attenuation and geometrical spreading were accounted for in the same way as the moment determination. For attenuation correction the Q model MM8 described by *Anderson et al.* [1965] was used. The radiation pattern was also taken into account, and *Wu's* [1966] procedure was used in integrating around the source on a unit sphere. The energy was estimated from the spectral density as follows:

$$E_p = \frac{1}{15\pi^2} \int_0^{\omega_0} \frac{\rho_s}{A^2(ih)} \frac{u_s^2(\omega)\ D^2(\omega)}{\mathrm{Amp}^2\ B^2(\omega)} \omega^2\, d\omega \quad (4)$$

where ρ_s is the density at the surface, u_s is the spectral density observed at the surface, D is the correction for attenuation, ω is frequency, $A(ih)$ is the correction for the radiation pattern, $(1/15\pi^2)$ is the factor resulting from the integration over a unit sphere, B is the correction for the effect of the crust and free surface, and $\mathrm{Amp} = u_s(\rho_s/I_f)^{1/2}$, where I_f = power per unit solid angle on a focal unit sphere. For frequencies between 0 and 1 hertz the integral in (4) simplifies to

$$E_p(1) = \frac{1.4}{T^3} \left[\frac{D(\omega_0)u(\omega_0)}{A(ih)\ \mathrm{Amp}\ B(\omega_0)} \right]^2 \quad (5)$$

The energy carried by the surface waves is automatically included in the body wave energy, since the integration was performed on a unit sphere around the source. $E_s = 10E_p(1)$ is taken as the estimate for the lower bound of seismically radiated energy. This value can be compared in Table 2 with $E_G(m_b)$, the energy estimated by the energy-magnitude relation [*Gutenberg and Richter*, 1956].

The magnitudes were based on amplitudes corrected for the radiation pattern of the short-period P waves recorded at Pasadena and Uppsala. The agreement between the energies estimated by the two methods is fair except for the two smallest shocks. This discrepancy is considered in a later section. For shallow events $E_p(1)$ could not be obtained because the 1-sec P wave did not reach the distant station of observation. The $E_p(1)$ determination was independent of the assumptions on which the magnitude determination and the energy-magnitude relation are based, and it allowed a check on the Gutenberg energy for shocks between 70 and 650 km depth. Both energy estimates are based on the P waves of the same seismographs. The agreement of the results obtained by the two methods indicates that there is no gross systematic error with depth in the Gutenberg energy determination for the region between 70 and 650 km. The Gutenberg energy estimate was therefore used for all strain determinations.

Both energy estimates are only a lower bound for the total energy, which could be an order of magnitude larger at all depths, as *Wu* [1966] suggests on the basis of his analyses of the S waves. In this case all the estimated strains and stresses would be an order of magnitude larger. We are more concerned, however, with the variations of apparent strain with depth than with its absolute value. To obtain a better estimate for the latter, we need a better energy determination. This improvement must come from local recordings of short-period waves that

SOUTH

propagated from the hypocenter up tl
slab.

Discussion

Apparent strain and stress. The
strain and apparent stress values for
quakes studied in this paper are given
2, columns 9 and 10. The apparent st
apparent stress for four additional ear
for which *Berckhemer and Jacob* [19
the moment were computed and inc
Table 2. The last column in the table
quality of the data for each earthqu
letter A indicates good data, and the
indicates less reliable results because
a poor fault plane solution or a smal

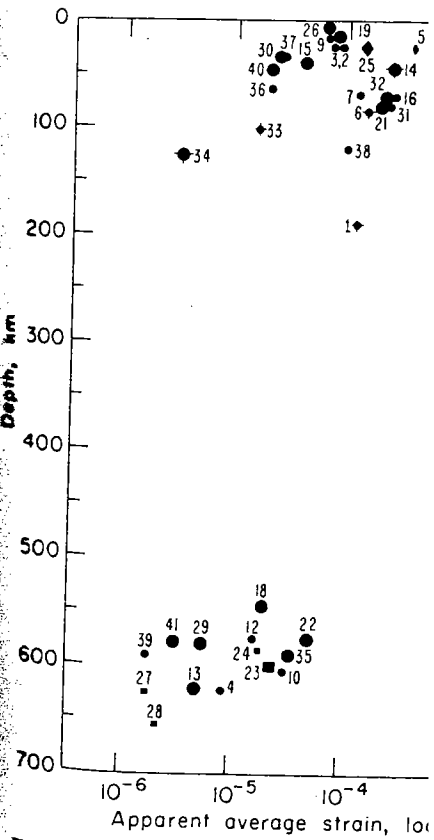

Fig. 2. Apparent average strain as a f
of depth. Squares indicate values obtaine
Berkhemer and Jacob [1968], crosses ov
circles mark events located near 18°S. The
bers correspond to the first column in T
and 2. Large symbols indicate reliable so
(quality A), small symbols less reliable so
(quality B). Diamonds as in Figure 1.

propagated from the hypocenter up the high Q slab.

Discussion

Apparent strain and stress. The apparent strain and apparent stress values for all earthquakes studied in this paper are given in Table 2, columns 9 and 10. The apparent strain and apparent stress for four additional earthquakes for which *Berckhemer and Jacob* [1968] give the moment were computed and included in Table 2. The last column in the table gives the quality of the data for each earthquake. The letter A indicates good data, and the letter B indicates less reliable results because of either a poor fault plane solution or a small size of the earthquake, so that the moment determination may be less accurate. The apparent strain and apparent stress values for all 41 earthquakes in Table 2 are plotted versus depth in Figures 2 and 3. Full circles with crosses indicate earthquakes located around 20°S, a portion of the seismic zone characterized by a complete lack of deep earthquakes.

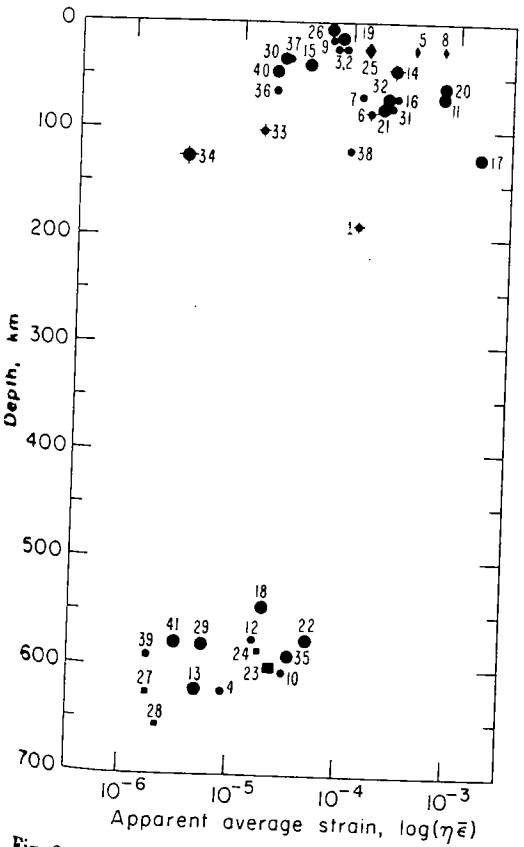

Fig. 2. Apparent average strain as a function of depth. Squares indicate values obtained from *Berkhemer and Jacob* [1968], crosses over full circles mark events located near 18°S. The numbers correspond to the first column in Tables 1 and 2. Large symbols indicate reliable solutions (quality A), small symbols less reliable solutions (quality B). Diamonds as in Figure 1.

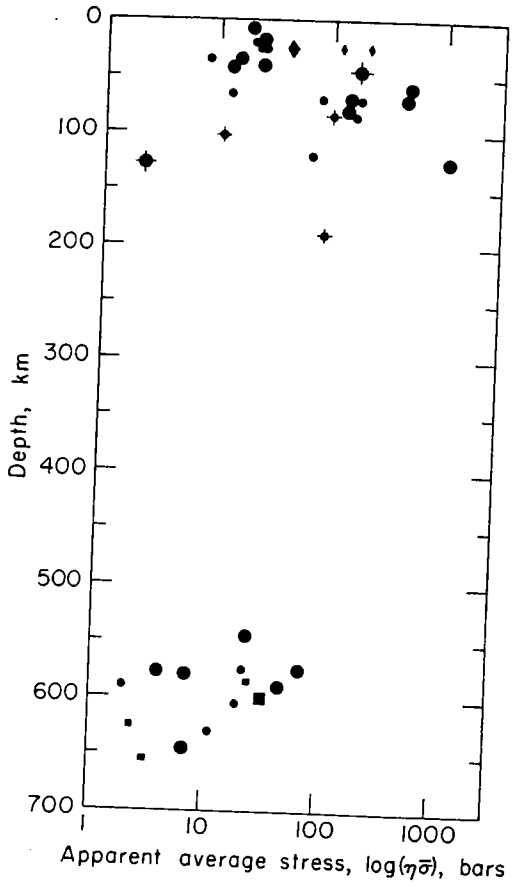

Fig. 3. Apparent average stress as a function of depth. Same symbols as in Figure 2.

An estimate of the errors that may be connected with points plotted in Figures 2 and 3 must be based on the accuracy with which the depth, the moment, and the energy are determined. The depths are taken from the USCGS and the IIS hypocentral locations and pP readings at Pasadena. For shallow earthquakes, if the fault dimensions exceed the hypocentral depth, the value for depth is more or less meaningless and the scatter is considerable. On the basis of agreement between moment obtained by

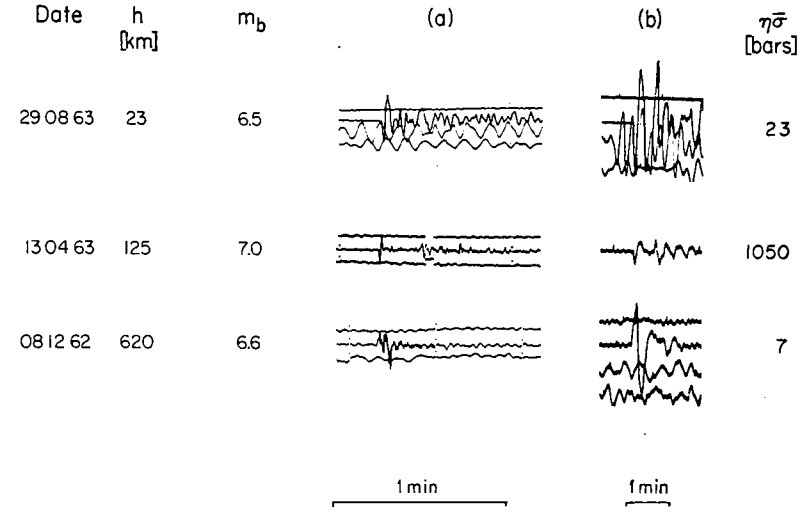

Fig. 4. Comparison of the vertical components of P waves for earthquakes at different depths recorded at Pasadena by (*a*) LP-Benioff and (*b*) LP Press-Ewing instruments.

surface and body wave analyses, the moment is believed to be accurate to within a factor of 2.5. The lower bound estimated for the seismic energy may be considerably different from the total seismic energy. This difference, however, may be accounted for by the seismic efficiency factor. The accuracy we are concerned with here is only the accuracy in estimating a consistent lower bound, since we are mainly concerned with *comparing* earthquakes. The agreement between the Gutenberg energy estimate and the estimate obtained by spectral density, is taken as an estimate of the relative accuracy of the energy values—on the average within a factor of 3. In the worst case the apparent strain values of a single shock could therefore be wrong by an order of magnitude. The mean error, however, is smaller. The apparent strain (stress) versus depth pattern in Figures 2 and 3 is believed to be significant.

To evaluate the changes of apparent strain (stress) with depth in a typical portion of the South American deep seismic zone, we must exclude the earthquakes with hypocenters outside this zone (diamond symbols) and those located in the peculiar region around 20°S (full circle with cross). Then we see that from the surface downward the pattern is one of rapid increase of apparent stress in the first 100 km. Around that depth a mean value of 270 bars and a largest value of about 1 kb is reached. With greater depth the apparent stress seems to decrease again. Unfortunately, there are no data available for intermediate depths because no earthquakes occur in that part of the South American seismic zone. From limited data on other trench systems it appears that the decrease occurs gradually. At great depths the apparent stresses reach a minimum with values comparable to the ones at the free surfaces (~20 bars).

For a qualitative evaluation of evidence for the relatively high apparent stresses around 100 km depth, examples of long-period seismograms are shown in Figure 4. The hypocenters were at depths of 0, 125, and 600 km, respectively. One can observe by inspection that the earthquake with $h = 125$ km radiated strong high-frequency and weak low-frequency waves compared with both the shallow and deep examples. The energy estimate is strongly dependent on the high-frequency content, and the moment estimate is dependent on the low-frequency content. The ratio of high- to low-frequency spectral amplitude, energy to moment, is a direct measure of the apparent strain (stress) in the source region. The apparent stress for the earthquake at a depth of 125 km is approximately 70 times higher than the apparent stresses in the source regions for the other two examples.

The diamond-shaped symbols in Figures 1, 2,

and 3 indicate shallow earthquakes lo
considerable distance landward from th
The hypocenters of these events do not
the general zone of seismic activity. The
earthquakes located in the main unc
zone have low apparent stresses, suggest
the breaks occur along well-developed a
tively well-lubricated fault zones.
earthquakes located outside the main zo
mond symbols) have high apparent
which may suggest that they occur al
well-developed fault surfaces.

Figure 5 represents another way of
at the same data, the seismic momer
plotted as a function of the body wave
tude. The line through the data is the t
cal curve obtained by *Brune and King*
This line is still a very good fit. As was
out by *Wyss and Brune* [1968], data
falling above this line correspond to eart
of low stresses in their source region a
points below this line indicate high
The division is very clear. The deep eart
fall above the line, and the shocks o
mediate depth fall below it.

Seismic efficiency and source dim
Since the apparent stress is a product
seismic efficiency and the average stress
source region, it is a question which of
factors is responsible for the variation
apparent stress with depth.

It is impossible to determine the seism
ciency without additional measurement
source region, such as measurements
dissipated energy, of the total elastically
energy, or of the source dimensions. If b
apparent stress $\eta\langle\sigma\rangle$ and the stress dro
available, an upper bound for the effici
may be estimated. To obtain the stress
is necessary to be able to estimate the
dimensions or the displacements associat
the dislocation. *Berkhemer and Jacob*
have obtained the stress drops of six
American shocks by assuming a rupture
ity at the source. Their estimate of stre
was based on a comparison of measured
tude spectral density of the P wave w
spectral density of propagating rupture
The total stress, for which the apparent
is a lower bound, must be at least as l
the stress drop. From a comparison of
hemer and Jacob's results for stress dro

and 3 indicate shallow earthquakes located at considerable distance landward from the trench. The hypocenters of these events do not fall into the general zone of seismic activity. The shallow earthquakes located in the main underthrust zone have low apparent stresses, suggesting that the breaks occur along well-developed and relatively well-lubricated fault zones. Shallow earthquakes located outside the main zone (diamond symbols) have high apparent stresses, which may suggest that they occur along less well-developed fault surfaces.

Figure 5 represents another way of looking at the same data, the seismic moment being plotted as a function of the body wave magnitude. The line through the data is the theoretical curve obtained by *Brune and King* [1967]. This line is still a very good fit. As was pointed out by *Wyss and Brune* [1968], data points falling above this line correspond to earthquakes of low stresses in their source region and data points below this line indicate high stresses. The division is very clear. The deep earthquakes fall above the line, and the shocks of intermediate depth fall below it.

Seismic efficiency and source dimensions. Since the apparent stress is a product of the seismic efficiency and the average stress in the source region, it is a question which of the two factors is responsible for the variation of the apparent stress with depth.

It is impossible to determine the seismic efficiency without additional measurement in the source region, such as measurements of the dissipated energy, of the total elastically released energy, or of the source dimensions. If both the apparent stress $\eta\langle\sigma\rangle$ and the stress drop τ are available, an upper bound for the efficiency η may be estimated. To obtain the stress drop it is necessary to be able to estimate the source dimensions or the displacements associated with the dislocation. *Berkhemer and Jacob* [1968] have obtained the stress drops of six South American shocks by assuming a rupture velocity at the source. Their estimate of stress drop was based on a comparison of measured amplitude spectral density of the P wave with the spectral density of propagating rupture models. The total stress, for which the apparent stress is a lower bound, must be at least as large as the stress drop. From a comparison of Berckhemer and Jacob's results for stress drop with the apparent stress, we can obtain an approximate upper bound for the efficiency.

Since $\sigma_2 \geq 0$ and $\tau \leq \sigma_1$,

$$\eta\langle\sigma\rangle = \eta\,\frac{\sigma_1 + \sigma_2}{2} \geq \eta\,\frac{\sigma_1}{2} \geq \eta\,\frac{\tau}{2}$$

$$\eta \leq \frac{2\eta\langle\sigma\rangle}{\tau} = \eta_{\max} \tag{6}$$

The maximum of the seismic efficiency is equal to the actual efficiency if the stress drops to zero. When melting occurs at the dislocation surface, the stress may indeed drop almost to zero, and the maximum efficiency, particularly for large shocks, may be not too different from the actual efficiency.

Berckhemer and Jacob determined stress drops for two models, one assuming a rupture

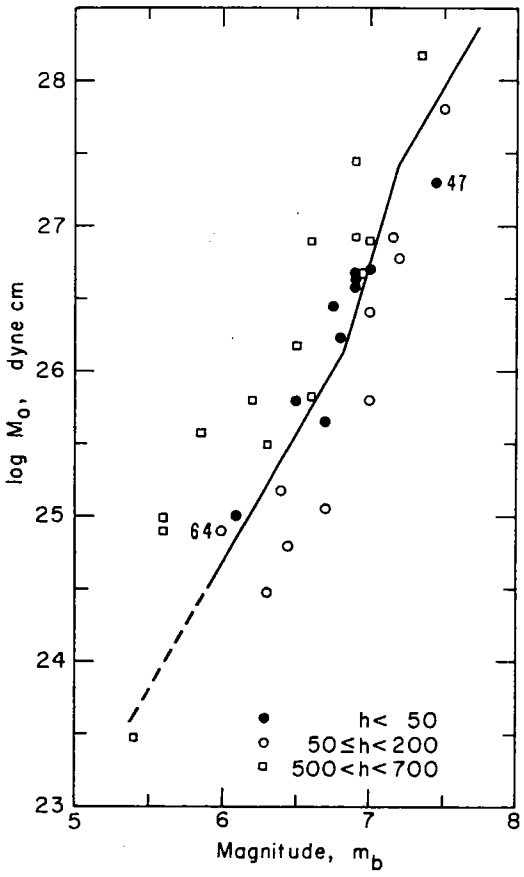

Fig. 5. Seismic moment as a function of body wave magnitude. Numbers near two events indicate depth in kilometers.

TABLE 3. Maximum Efficiency and Dislocation Area

Event	h	Stress Drop τ_1, bars	Stress Drop τ_2, bars	Maximum Efficiency $\eta_{1\,max}$	Maximum Efficiency $\eta_{2\,max}$	m_b	Dislocation Area F_1, km²	Dislocation Area F_2, km²
17	125	24,000	8,500	0.09	0.25	7.0	3.	6.
21	80	6,900	2,450	0.04	0.11	7.0	20.	40.
22	575	1,200*	425*	0.12	0.33	7.0	140.*	280.*
23	600	920*	325*	0.07	0.2	6.3	20.*	40.*
24	585	30*	11*	>1.	>1.	5.4	7.*	14.*
27	626	270*	95*	0.02	0.05	5.6	20.*	40.*
28	655	220*	78*	0.03	0.08	5.6	20.*	40.*
35	590	250*	89*	0.38	1.	6.6	34.*	68.*

* *Berckhemer and Jacob* [1968].

velocity of 2.5 km/sec, called τ_1, and one assuming 3.53 km/sec, called τ_2. The values given for η_{1max} and η_{max} in Table 3 suggest that for deep earthquakes the level of maximal seismic efficiency may be around 10% and that it is a function of magnitude. The dependence of efficiency on magnitude is shown by the plot of the apparent stress of deep earthquakes versus body wave magnitude in Figure 6*a*. It is very clear that the apparent stress of deep earthquakes is a function of magnitude. On the map of South America the deep earthquakes plot as two groups, triangles and circles in Figure 6*a*, epicenters 4 and 18 being somewhat apart from the others. Each group separately shows approximately the same dependence of apparent stress on magnitude. The hypocenters of each cluster are located very close to each other, and magnitude does not vary systematically with depth. The total stress can therefore be assumed to be roughly constant in each group. Under this assumption the efficiency must vary with magnitude. It may be significant that the earthquakes of the northernmost group display consistently the highest apparent stresses at all magnitudes, but at this point there are not enough data to make a convincing case for this regional difference. The straight line in Figure 6*a* therefore is an average least-squares fit to all data except one anomalous point, and the equation for it is

$$\log (\eta\langle\sigma\rangle) = 0.8m_b - 4.1 \qquad \begin{matrix} 500\text{ km} < h \\ 5.5 < m_b < 7.5 \end{matrix} \qquad (7)$$

If the average stress is assumed to be a constant, the slope of 0.8 indicates the variation of efficiency with magnitude is

$$\log \eta = 0.8m_b + c$$

To fit a straight line to the data in Figure 6*a* is a crude approximation. It implies that earthquakes of sufficient size, say around $m_b = 8.0$, will be 100% efficient. This is impossible, and a curve decreasing in slope with increasing magnitude would be a more realistic approximation.

The above results are valid only for deep shocks. Intermediate-depth earthquakes are more difficult to analyze because the apparent stress increases rapidly with depth. The data for intermediate shocks are plotted in Figure 6*b*. Earthquakes located in the anomalous region around 20°S are omitted. The range of magnitudes covered is not large enough to warrant definite conclusions, but the efficiency of intermediate earthquakes may well be a strong function of magnitude. The dislocation area of two shocks at intermediate depth were determined by the method of *Berckhemer and Jacob* [1968], and the stress drops, as well as the maximal efficiencies, were estimated (Table 3). The maximal efficiencies of these earthquakes at intermediate depth are approximately the same as those for deep earthquakes.

The apparent stresses of shallow shocks analyzed in this study do not vary significantly with magnitude. This observation is in agreement with the study by *King* [1969], who found a very small dependence of efficiency on magnitude for shallow shocks.

The dependence of apparent stres magnitude could be caused by two thing the physics of the source or a system in the analysis due to overestimation of or underestimation of energy for small The seismic moment as an error sou safely be discarded. The seismic energ ever, could indeed be systematically u mated for small shocks. In determinin we considered periods only down to 1 the largest events the periods with t energy contribution are included in this For small shocks the waves with periods than 1 sec carry a larger fraction of t energy than those neglected periods do f shocks. Comparison of $E_p(1)$ with the berg energy E_a (Table 2) shows tha corrected for this effect. Yet it may the correction is not large enough. H quency recordings of waves propagating high Q zone under island arcs, as repo Oliver *and Isacks* [1967], may furni answer to this problem. Until more studies are completed, the energy under tion cannot be ruled out as a possible sys error.

Earthquakes at great depth could b ated with dehydration of hydrous m [*Raleigh and Paterson*, 1965; *Isacks* 1968] or with melt on the shear plane [*O* 1960; *Griggs and Baker*, 1969; *Savage*, In the latter case a very simple physical ation for the varying efficiency co fered. With increasing magnitude the a of melt and the amount of energy lost by increase in rough proportion to the the earthquake dimensions. The amo available elastic energy, however, increase third power of the earthquake dime This would mean that for large shocks a s portion of energy disappears into hea ciency consequently increases with incr gnitude.

To make the data presented in Figure 3 mogeneous, the apparent average stres rmalized to magnitude 7.0. It was as that (7) holds not only for deep but al termediate earthquakes, and all shocks pocenter below 45 km were normalize ding to (7). For shallow shocks no c was considered necessary. The res wn in Figure 7. The symbols are the

The dependence of apparent stress versus magnitude could be caused by two things, either the physics of the source or a systematic bias in the analysis due to overestimation of moment or underestimation of energy for small shocks. The seismic moment as an error source can safely be discarded. The seismic energy, however, could indeed be systematically underestimated for small shocks. In determining $E_p(1)$, we considered periods only down to 1 sec. For the largest events the periods with the main energy contribution are included in this interval. For small shocks the waves with periods shorter than 1 sec carry a larger fraction of the total energy than those neglected periods do for large shocks. Comparison of $E_p(1)$ with the Gutenberg energy E_G (Table 2) shows that E_G is corrected for this effect. Yet it may be that the correction is not large enough. High-frequency recordings of waves propagating up the high Q zone under island arcs, as reported by *Oliver and Isacks* [1967], may furnish the answer to this problem. Until more detailed studies are completed, the energy underestimation cannot be ruled out as a possible systematic error.

Earthquakes at great depth could be associated with dehydration of hydrous minerals [*Raleigh and Paterson*, 1965; *Isacks et al.*, 1968] or with melt on the shear plane [*Orowan*, 1960; *Griggs and Baker*, 1969; *Savage*, 1969]. In the latter case a very simple physical explanation for the varying efficiency could be offered. With increasing magnitude the amount of melt and the amount of energy lost by melting increase in rough proportion to the square of the earthquake dimensions. The amount of available elastic energy, however, increases with the third power of the earthquake dimensions. This would mean that for large shocks a smaller proportion of energy disappears into heat. The efficiency consequently increases with increasing magnitude.

To make the data presented in Figure 3 more homogeneous, the apparent average stress was normalized to magnitude 7.0. It was assumed that (7) holds not only for deep but also for intermediate earthquakes, and all shocks with hypocenter below 45 km were normalized according to (7). For shallow shocks no correction was considered necessary. The result is shown in Figure 7. The symbols are the same as in Figures 2 and 3. The general pattern of Figures 2 and 3 is preserved and the scatter is reduced. The averages of the normalized apparent stresses are 18 bars at $h \leq 45$ km, 380 bars at 45 km $< h \leq$ 125 km, and 44 bars at 450 km $< h <$ 660 km. These values apply for a magnitude 7.0 event for which at all depths the efficiency is estimated to be less than 0.1. If the stress drops almost to zero, the efficiency will be close to 0.1.

The apparent strain is the energy density in the source region. The fact that an earthquake of a given magnitude has larger strains around 100 km depth than at the surface implies that the source dimensions at 100 km depth are much smaller. The dislocation areas were roughly estimated by the method of *Berckhemer and Jacob* [1968] for two shocks around 100 km

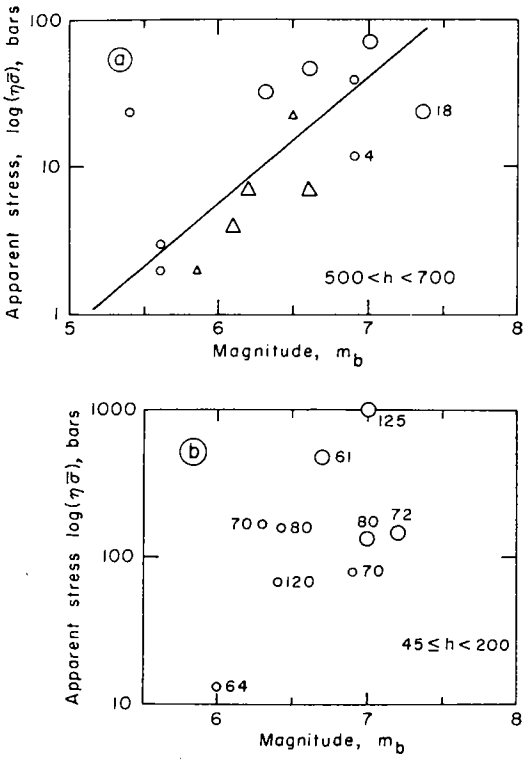

Fig. 6. Apparent stress as a function of body wave magnitude. (*a*) For deep shocks. Triangles indicate earthquakes located around 27°S; circles represent earthquakes between 8° and 15°S. Large symbols again indicate reliable solutions, small symbols less reliable ones. Numbers near two circles are event numbers. (*b*) For intermediate earthquakes, numbers indicate depth in kilometers.

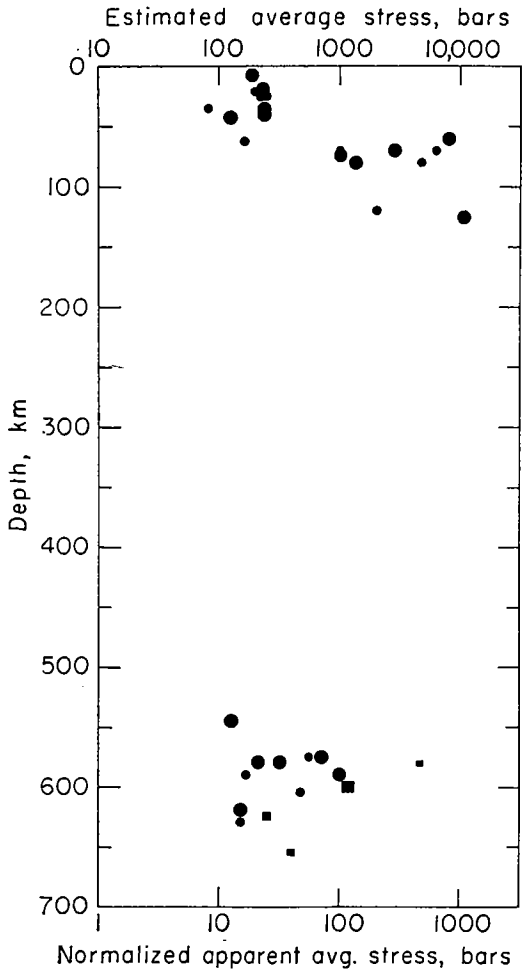

Fig. 7. The bottom scale gives the apparent stress normalized to $m_b = 7.0$. The top scale gives an approximate estimate for the total average stress. Same symbols as in Figure 2. Data outside typical seismic zone not shown.

depth. The fault dimensions of these magnitude 7.0 events are estimated to be between 1 and 6 km. These values are surprisingly small, but they agree with several observations listed by *Iida* [1959]. The high stresses correspond well to the breaking stresses of crustal rocks. The estimated stresses of 3 kb at 100 km depth also agree well with the pressure a sinking slab exerts on the lithosphere. *McKenzie* [1969] estimated density differences between the mantle and the descending slab as due to temperature differences and obtained a minimum estimate of 2.5 kb for the stresses that could be accumulated in the slab.

Comparison with other trenches. *Oliver* [illegible] *Isacks* [1967] studied the high-frequency [illegible] tent of S and P waves from deep earthqua[illegible] in the Tonga-Fiji region on the records of l[illegible] stations. They found that waves traveling [illegible] the deep seismic zone were much less att[illegible] ated than waves traveling in the surround[illegible] mantle. From these observations they conclu[illegible] that cold lithospheric material was plung[illegible] underneath the island arc and remaining r[illegible] tively cold down to the depth of the dee[illegible] earthquakes. A corollary is that low attenua[illegible] for the deepest earthquakes can only be [illegible] served if the descending slab of lithospher[illegible] continuous and has the high Q property all a[illegible] its length. From limited data it appears tha[illegible] other trench systems the apparent stresses [illegible] increase rapidly with depth, reach a maxim[illegible] and decrease again at greater depth. Stre[illegible] associated with earthquakes at intermedi[illegible] depths in the Tonga-Kermadec trench h[illegible] intermediate values between the high stre[illegible] at 100 km depth and the low stresses aro[illegible] 600 km depth. This may indicate that in t[illegible] island arc the material at intermediate de[illegible] has intermediate values of strength.

Kasahara [1957] has estimated the so[illegible] volume of shallow and deep shocks in Ja[illegible] Dividing the Gutenberg energy by the vol[illegible] he obtained energy density. This value co[illegible] sponds to

$$\eta(\epsilon_1^2 - \epsilon_2^2) = \eta(\epsilon_1 - \epsilon_2)(\epsilon_1 + \epsilon_2) = 2\eta$$

and is not quite comparable to the appa[illegible] strain determined in this study. Even tho[illegible] Kasahara's study was confined to a diff[illegible] island arc, his results for shallow and [illegible] shocks are in approximate agreement wit[illegible] results presented here. Kasahara has not, [illegible] ever, analyzed shocks in the critical depth [illegible] around 100 km.

If a ray should propagate down the rigid [illegible] Q slab [*Oliver and Isacks*, 1967] and up an[illegible] such rigid slab to a recording station, the [illegible] frequencies would fail to be filtered in the [illegible] velocity zone. This would lead to a rel[illegible] overestimate of the energy and hence to [illegible] overestimate of the apparent average s[illegible] relative to earthquakes at greater depth. In [illegible] study, therefore, care was taken not to co[illegible] ray paths propagating down or up a slab.

Ocean floor consumption. The two var[illegible]

[illegible]hich control the strength of rocks in th[illegible] [illegible]re pressure and temperature. The cha[illegible] [illegible]lastic properties of material present [illegible] [illegible]thosphere and mantle are small and [illegible] [illegible]eglected, with one important excepti[illegible] [illegible]ehavior of serpentinite described by [illegible] [illegible]nd Paterson* [1965]. Under confining p[illegible] [illegible] 5 kb and low temperature, serpentinit[illegible] [illegible]gh strength. Above 300° to 500°C de[illegible] [illegible]n occurs and the serpentinite loses s[illegible] [illegible]ry rapidly. In general, increasing press[illegible] [illegible]eases the strength, increasing temperat[illegible] [illegible]eases it. In particular, at the depth [illegible] [illegible]w-velocity channel, around 100 km, th[illegible] [illegible]erature-pressure conditions are such th[illegible] [illegible]aterial is very likely to be partly [illegible] [illegible]Anderson and Sammis*, 1969] and wil[illegible] [illegible]tremely low strength. In the zone o[illegible] [illegible]rthquakes, however, the present analy[illegible] [illegible]cates that the material around 100 k[illegible] [illegible]ry high strength. The hydrostatic pres[illegible] [illegible]e descending slab and the neighboring [illegible] [illegible] approximately the same. It is clear th[illegible] [illegible]mperatures must be different.

[illegible]This result supports the hypothesis of [illegible] [illegible]or consumption. As the lithosphere p[illegible] [illegible]wnward, the pressure increases insta[illegible] [illegible]dy. Because of the low heat conductiv[illegible] [illegible]e material, the slab is heated very slow[illegible] [illegible]e surrounding mantle. Simple models [illegible] [illegible]mperature distribution in a descending[illegible] [illegible]dicate that the slab can stay relatively[illegible] [illegible]th respect to the surrounding mantle [illegible] [illegible] the depth of the deepest earthquakes [illegible] [illegible]Mazie*, 1969]. Two lines of evidence in[illegible] [illegible]t earthquakes deeper than about 60 k[illegible] [illegible]e account for the slip of the descending[illegible] [illegible]h respect to the adjacent mantle. [illegible] [illegible]68] showed that the slip rate computed [illegible] [illegible]sum of the seismic moments for interme[illegible] [illegible] deep earthquakes is much too smal[illegible] [illegible]cluded that creep along a weak boun[illegible] [illegible]ween the mantle and the lithospheric [illegible] [illegible]l take place. In addition, *Isacks et al.* [illegible] [illegible]Isacks and Molnar* [1969] have shown [illegible] [illegible]fault planes for intermediate and deep e[illegible] [illegible]kes are not parallel to the slip directi[illegible] [illegible] slab. They showed that, instead, the [illegible] [illegible]or the tension axis is parallel to the [illegible] [illegible] stresses released by earthquakes are sti[illegible] [illegible]gated along the slab as it is pulle[illegible] [illegible]d down into the mantle. The amou[illegible]

which control the strength of rocks in the earth are pressure and temperature. The changes of elastic properties of material present in the lithosphere and mantle are small and can be neglected, with one important exception, the behavior of serpentinite described by *Raleigh and Paterson* [1965]. Under confining pressure of 5 kb and low temperature, serpentinite shows high strength. Above 300° to 500°C dehydration occurs and the serpentinite loses strength very rapidly. In general, increasing pressure increases the strength, increasing temperature decreases it. In particular, at the depth of the low-velocity channel, around 100 km, the temperature-pressure conditions are such that the material is very likely to be partly melted [*Anderson and Sammis*, 1969] and will have extremely low strength. In the zone of deep earthquakes, however, the present analysis indicates that the material around 100 km has very high strength. The hydrostatic pressure in the descending slab and the neighboring mantle is approximately the same. It is clear that the temperatures must be different.

This result supports the hypothesis of ocean floor consumption. As the lithosphere plunges downward, the pressure increases instantaneously. Because of the low heat conductivity of the material, the slab is heated very slowly by the surrounding mantle. Simple models of the temperature distribution in a descending slab indicate that the slab can stay relatively cool with respect to the surrounding mantle down to the depth of the deepest earthquakes [*McKenzie*, 1969]. Two lines of evidence indicate that earthquakes deeper than about 60 km do not account for the slip of the descending slab with respect to the adjacent mantle. *Brune* [1968] showed that the slip rate computed from the sum of the seismic moments for intermediate and deep earthquakes is much too small. He concluded that creep along a weak boundary between the mantle and the lithospheric slab must take place. In addition, *Isacks et al.* [1968] and *Isacks and Molnar* [1969] have shown that the fault planes for intermediate and deep earthquakes are not parallel to the slip direction of the slab. They showed that, instead, the pressure or the tension axis is parallel to the slab. The stresses released by earthquakes are stresses propagated along the slab as it is pulled or pushed down into the mantle. The amount of stress the material in the slab is able to accumulate before it breaks is only a function of the local strength of material in the slab. The present results suggest that, as the slab plunges down, the strength of the lithosphere increases first, and when the increase in temperature becomes appreciable, around 150 km, weakening starts. The strength then decreases until at depths around 600 km the strength is almost as small as the strength at the surface. At still greater depth the slab material can no longer support stresses large enough to produce earthquakes, and it blends into the rest of the mantle. The South American slab is demonstrated to be in a thermal steady state along its length. The length of this slab is not determined by the age of the present consumption site or by a change in mantle properties at this depth but is a function only of the temperature and pressure conditions in the mantle and the local consumption rate. It will be important to determine, in island arcs where the seismic activity is continuous from the surface to great depths, whether the decrease in strength is sudden or gradual, that is, whether the mechanism of brittle fracture proposed by *Raleigh and Paterson* [1965] is applicable.

It is now very interesting to determine the stresses associated with the lower terminating earthquakes in trench systems where the deepest activity occurs at intermediate depth. If such earthquakes indicate low strength, i.e., apparent stresses of the order of 20 to 50 bars, one can conclude the slab is heated at its lower termination to the extent that it cannot support stresses and blends with the mantle. This conclusion implies that the slab has reached a thermal steady state, and its short length must be due to a slow consumption rate. If, on the other hand, such lower terminating earthquakes of intermediate depth yield intermediate to high values of strength, i.e, apparent stresses between 100 and 1000 bars, the slab would not be heated enough to terminate the earthquake activity. In this case the shortness of the slab would have to be a function of the time during which the trench was active. The shorter the slab with relatively high-stress bottom, the younger the consuming system.

In the South American slab there is an anomalous region between 13° and 19°S. In this part the deepest earthquakes large enough to yield

fault plane solutions and moment determinations occur at depths of about 120 km, and deep earthquakes do not occur at all [*Barazangi and Dorman*, 1969]. The stress analysis of this region showed that shocks around 100 km depth have anomalously low stresses that are comparable to the stresses of very deep earthquakes in the other parts of the descending slab. These events are marked by full circles with a superimposed cross in Figures 2, 3, and 4. The absence of deep-focus earthquakes, together with the low strength of the slab at 100 km depth, suggests that this part of the slab may be heated faster than any other part. Seismicity off the coast of South America indicates only one rigid plate between the equator and 40°S. The consumption rate therefore cannot drop and increase again from north to south along the trench. The marked change in direction of the trench around 17°S may be interpreted as the meeting point of two trenches, the convex Peruvian trench and the straight Chilean trench. The descending slab may be broken up in this discontinuous region. The surrounding mantle may then partially penetrate the slab material, which would be heated far more efficiently than an ordinary portion of the slab. The stresses at intermediate depth would then indicate low strength, and stresses for deep earthquakes will not accumulate.

Conclusions

An attempt was made to determine the total stress in the source region of earthquakes in the South American seismic zone. It is impossible to obtain rigorously the total shear stress causing earthquakes because the seismic efficiency cannot be known without additional measurements in the source region. What can be determined is the apparent stress, the product of average stress and seismic efficiency. A comparison of the maximal seismic efficiency at different depths allows the conclusion that the variations with depth of apparent stress closely reflect variations of total stress. It was demonstrated that variations of more than an order of magnitude exist between the ratios of short-period to long-period waves radiated by earthquakes at different depths. From this ratio the apparent average stress in the source region was obtained. The apparent average stresses reach a maximum around 100 km depth. The mean value for a magnitude 7.0 earthquake at this depth is 380 bars, an order of magnitude larger than the values at shallow and 600 km depth.

Under the assumption of a rupture velocity at the source, the stress drop associated with deep earthquakes can be obtained. The stress drops at intermediate depth are approximately an order of magnitude higher than those at shallow and great depths. From a comparison of stress drop with apparent stress an upper bound can be put on the seismic efficiency. The seismic efficiency defined at teleseismic distances is of the order of 10% and does not vary significantly with depth.

On these grounds the total shear stresses associated with earthquakes are estimated to be at least 200 bars between the surface and 40 km, 3 kb around 100 km depth, and 440 bars at 600 km depth. Changes of the average stress reflect changes of the strength of the earthquake zone as a function of depth. The strength increases with increasing depth and reaches a maximum at about 100 km. At greater depth the strength decreases again until at 600 km it reaches about the same value as at the surface. This pattern is believed to be an expression of the temperature-pressure conditions in a slab of lithosphere which is plunging into the mantle. With increasing pressure the strength increases until the slab is heated enough to be progressively weakened by increasing temperature. At depths below about 650 km the South American slab becomes so weak that no earthquakes can occur. The apparent average stresses are a good test for the nature of the bottom cutoff of an island arc. If the deepest earthquakes in a given island arc indicate high stresses, the island arc is not in thermal steady state; i.e., it is young. If the deepest earthquakes indicate stresses comparable to those at zero depth, the island arc is in thermal steady state.

The concave bend in the South American trench around latitude 17°S is associated with a discontinuity of deep seismic activity and with low stresses at 100 km depth. The South American trench should perhaps be viewed as two trenches, the Chilean and the Peruvian, meeting at 17°S.

The high stresses and strains between 45 and 120 km depth indicate high-energy density in the source region. A comparatively small volume is needed to produce an earthquake of

given size. At these depths the fault ... of a magnitude 7.0 event are estimate... from 1 to 10 km.

Acknowledgments. I am indebted ... Brune, who had continuous interest in ... and provided very helpful suggestions ... cism in numerous discussions. Thanks ... given to J. N. Brune, D. P. McKenzie, ... Archambeau for critically reading the ... and making helpful suggestions. I am ... debted to B. R. Julian and D. L. Ande... kindly furnished the program which t... rays back to the source.

This study was supported by National ... Foundation grant GA 11332.

References

Aki, K., Generation and propagation of ... from the Niigata earthquake of June ... 2. Estimation of earthquake moment, ... energy, and stress strain drop from the ... spectrum, *Bull. Earthquake Res. Inst. Univ., 44*, 73–88, 1966.

Anderson, Don L., Ari Ben-Menahem, and ... B. Archambeau, Attenuation of seismic ... in the upper mantle, *J. Geophys. Res.*, ... 1448, 1965.

Anderson, Don L., and C. G. Sammis, ... melting in the upper mantle, *Phys. Planet. Interiors*, in press, 1969.

Archambeau, Charles B., Elastodynamic ... theory, Ph.D. thesis, California Insti... Technology, Pasadena, 1964.

Barazangi, G., and T. Dorman, World sei... maps compiled from ESSA, Coast and G... Survey, epicenter data 1961–1967, *Bull. S... Soc. Am., 59*, 369–380, 1969.

Ben-Menahem, Ari, Observed attenuation ... values of seismic surface waves in the ... mantle, *J. Geophys. Res., 70*, 4641–4651, ...

Ben-Menahem, Ari, and D. G. Harkrider, ... tion patterns of seismic surface waves ... buried dipolar point sources in a flat str... earth, *J. Geophys. Res., 59*, 2605–2620, 19...

Ben-Menahem, Ari, S. W. Smith, and Ta-Teng, A procedure for source studies from ... trums of long-period seismic body waves, *Seismol. Soc. Am., 55*, 203–235, 1965.

Berckhemer, H., and K. H. Jacob, Investig... of the dynamical process in earthquake fo... analyzing the pulse shape of body waves, ... Sci. Rept., Contract AF61(052)-801*, 85 pp., ... ute of Meteorology and Geophysics, Unive... of Frankfurt, Germany, 1968.

Brune, J. N., Seismic moment, seismicity, ... rate of slip along major fault zones, *J. Geo... Res., 73*, 777–784, 1968.

Brune, J. N., and Chi-Yu King, Excitation ... mantle Rayleigh waves of period 100 sec ... function of magnitude, *Bull. Seismol. Soc. ... 57*, 1355–1366, 1967.

given size. At these depths the fault dimensions of a magnitude 7.0 event are estimated to range from 1 to 10 km.

Acknowledgments. I am indebted to J. N. Brune, who had continuous interest in this work and provided very helpful suggestions and criticism in numerous discussions. Thanks are also given to J. N. Brune, D. P. McKenzie, and C. B. Archambeau for critically reading the manuscript and making helpful suggestions. I am also indebted to B. R. Julian and D. L. Anderson, who kindly furnished the program which traced the rays back to the source.

This study was supported by National Science Foundation grant GA 11332.

References

Aki, K., Generation and propagation of *G* waves from the Niigata earthquake of June 16, 1964, 2, Estimation of earthquake moment, released energy, and stress strain drop from the *G* wave spectrum, *Bull. Earthquake Res. Inst., Tokyo Univ., 44,* 73–88, 1966.

Anderson, Don L., Ari Ben-Menahem, and Charles B. Archambeau, Attenuation of seismic energy in the upper mantle, *J. Geophys. Res., 70,* 1441–1448, 1965.

Anderson, Don L., and C. G. Sammis, Partial melting in the upper mantle, *Phys. Earth Planet. Interiors,* in press, 1969.

Archambeau, Charles B., Elastodynamic source theory, Ph.D. thesis, California Institute of Technology, Pasadena, 1964.

Barazangi, G., and T. Dorman, World seismicity maps compiled from ESSA, Coast and Geodetic Survey, epicenter data 1961–1967, *Bull. Seismol. Soc. Am., 59,* 369–380, 1969.

Ben-Menahem, Ari, Observed attenuation and *Q* values of seismic surface waves in the upper mantle, *J. Geophys. Res., 70,* 4641–4651, 1965.

Ben-Menahem, Ari, and D. G. Harkrider, Radiation patterns of seismic surface waves from buried dipolar point sources in a flat stratified earth, *J. Geophys. Res., 59,* 2605–2620, 1964.

Ben-Menahem, Ari, S. W. Smith, and Ta-Liang Teng, A procedure for source studies from spectrums of long-period seismic body waves, *Bull. Seismol. Soc. Am., 55,* 203–235, 1965.

Berkhemer, H., and K. H. Jacob, Investigation of the dynamical process in earthquake foci by analyzing the pulse shape of body waves, *Final Sci. Rept., Contract AF61(052)-801,* 85 pp., Institute of Meteorology and Geophysics, University of Frankfurt, Germany, 1968.

Brune, J. N., Seismic moment, seismicity, and rate of slip along major fault zones, *J. Geophys. Res., 73,* 777–784, 1968.

Brune, J. N., and Chi-Yu King, Excitations of mantle Rayleigh waves of period 100 sec as a function of magnitude, *Bull. Seismol. Soc. Am., 57,* 1355–1366, 1967.

Bullen, K. E., *An Introduction to the Theory of Seismology,* Cambridge University Press, England, 1963.

Griggs, D. T., and D. W. Baker, The origin of deep-focus earthquakes, in *Properties of Matter,* p. 11, John Wiley & Sons, New York, 1969.

Gutenberg, B., and C. F. Richter, Magnitude and energy of earthquakes, *Ann. Geofis., 9,* 1–15, 1956.

Haskell, N., Total energy and energy spectral density of elastic wave radiation from propagating faults, *Bull. Seismol. Soc. Am., 54,* 1811–1841, 1964.

Iida, Kumizi, Earthquake energy and earthquake fault, *J. Earth Sci., Nagoya Univ., 7,* 98–107, 1959.

Isacks, B., and Peter Molnar, Focal mechanisms of deep and intermediate depth earthquakes and the dynamics of the lithosphere (abstract), *EOS, Trans. Am. Geophys. Union, 50,* 2381, 1969.

Isacks, B., J. Oliver, and L. R. Sykes, Seismology and the new global tectonics, *J. Geophys. Res., 73,* 5855–5899, 1968.

Julian, B. R., and D. L. Anderson, Travel times, apparent velocities and amplitudes of body waves, *Bull. Seismol. Soc. Am., 58,* 339–366, 1968.

Kasahara, K., The nature of seismic origins as inferred from seismological and geodetic observations, *Bull. Earthquake Res. Inst., Tokyo Univ., 35* 473–532, 1957.

Keilis-Borok, V. I., *Investigation of the Mechanism of Earthquakes, Soviet Research in Geophysics,* vol. *4,* American Geophysical Union and Consultants Bureau Enterprises, New York, 1960.

Khattrie, K. N., Focal mechanism of the Brazil deep focus earthquake of November 3, 1965, from the amplitude spectra of isolated *P* waves, *Bull. Seismol. Soc. Am., 59,* 691–704, 1969.

King, Chi-Yu, Seismic efficiency, *J. Geophys. Res., 74,* 1702–1703, 1969.

Maruyama, T., On the force equivalent of dynamic elastic dislocations with reference to the earthquake mechanism, *Bull. Earthquake Res. Inst., Tokyo Univ., 41,* 464–486, 1963.

McKenzie, Dan P., Speculations on the consequences and causes of plate motions, *Geophys. J., 18,* 1–32, 1969.

Oliver, Jack, and Bryan Isacks, Deep earthquake zones, anomalous structures in the upper mantle, and the lithosphere, *J. Geophys. Res., 72,* 4259–4275, 1967.

Orowan, E., Mechanism of seismic faulting in rock deformation, *A Symposium, Geol. Soc. Am. Mem., 79,* 323–345, 1960.

Raleigh, C. B., and M. S. Paterson, Experimental deformation of serpentinite and its tectonic implications, *J. Geophys. Res., 70,* 3965–3985, 1965.

Savage, J. C., A possible explanation of the orientation of fault planes for deep-focus earthquakes

(abstract), Annual meeting of the Seismological Society of America, 1969.
Stauder, W., Focal mechanisms for South American earthquakes, in preparation, 1970.
Stauder, W., and G. A. Bollinger, The *S*-wave project for focal mechanism studies: earthquakes of 1962, *Bull. Seismol. Soc. Am., 54,* 2199–2208, 1964.
Stauder, W., and G. A. Bollinger, The *S*-wave project for focal mechanism studies. earthquakes of 1963, *Bull. Seismol. Soc. Am., 56,* 6, 1363–1371, 1966.
Wickens, A. T., and T. H. Hodgson, Computer re-evaluation of earthquake mechanism solutions 1922–1962, *Publ. Dominion Obs., Ottawa 33,* 1967.
Wu, Francis T., Lower limit of the total energy of earthquakes and partitioning of energy among seismic waves, Ph.D. thesis, California Institute of Technology, Pasadena, 1966.
Wyss, M., and J. N. Brune, Seismic moment, stress, and source dimensions for earthquakes in the California-Nevada region, *J. Geophys. Res., 73,* 4681–4694, 1968.

(Received August 18, 1969.)

An Analysis o Sequence Us

P. W. BASHAM, D.

Division of Seismology

The Nevada Test Site (NTS) expl tributed over the magnitude range u studies of detection and identification shocks and other NTS explosions are the Canadian network ($12° \leq \Delta \leq$ aftershocks larger than m 3.6, but not can detect Rayleigh waves for all afte spectral ratio discriminants produce e similar body-wave magnitude NTS ex 50 km in longitude of the Yellowknif differences in aftershock and explosion

INTRODUCTION

It has recently been found that large ground nuclear explosions can influenc seismic activity near the shot point. I shown by *Ryall et al.* [1969] from a stu twenty-one Nevada Test Site explosions t shots larger than m 5.0 produce an incre seismicity for at least a day followin shot. *Healy and Hamilton* [1969] reporte post-shot activity continued for at least 3 following some of the largest explosions ar peared to be caused by movement on prev recognized fractures within about 10 km explosions and at focal depths from surf about 5 km.

The m 6.3 explosion Benham caused a stantial number of aftershocks, many of were large enough to be recorded at teles distances from the test site. The U.S. and Geodetic Survey (USCGS) 'Prelim Determination of Epicenters' lists fort earthquakes for the period between the Be first time on December 19, 1968, and Ja 29, 1969, with locations within a few tent a degree of the shot point. This series of shocks provides a unique opportunity to

[1] Contribution from the Dominion Observ No. 392.
[2] Order of authors drawn by lot.